Superfluid density and superconducting gaps of $RbFe_2As_2$ as a function of hydrostatic pressure

Z. Shermadini,[1,*] H. Luetkens,[1] A. Maisuradze,[1,2] R. Khasanov,[1] Z. Bukowski,[3,4] H.-H. Klauss,[5] and A. Amato[1]

[1]*Laboratory for Muon Spin Spectroscopy, Paul Scherrer Institute, CH-5232 Villigen PSI, Switzerland*

[2]*Physik-Institut der Universität Zürich, Winterthurerstrasse 190, CH-8057 Zürich, Switzerland*

[3]*Laboratory for Solid State Physics, ETH Zürich, CH-8093 Zürich, Switzerland*

[4]*Institute of Low Temperature and Structure Research, Polish Academy of Sciences, 50-422 Wroclaw, Poland*

[5]*Institut für Festkörperphysik, TU Dresden, D–01069 Dresden, Germany*

(Received 21 September 2012; revised manuscript received 5 November 2012; published 19 November 2012)

The superfluid density and superconducting gaps of superconducting $RbFe_2As_2$ have been determined as a function of temperature, magnetic field, and hydrostatic pressure by susceptibility and muon-spin spectroscopy measurements. From the data, fundamental microscopic parameters of the superconducting state like the London penetration depth λ, the gap values Δ, the upper critical field B_{c2}, and the Ginzburg-Landau parameter κ have been obtained. In accordance with earlier measurements the ratio of the superfluid density $n_s \propto \lambda^{-2}$ to the superconducting transition temperature $T_c = 2.52(2)$ K at ambient pressure is found to be much higher in the strongly hole-overdoped $RbFe_2As_2$ than in high-T_c Fe-based and other unconventional superconductors. As a function of pressure, T_c strongly decreases, at the rate of $T_c/dp = -1.32$ K GPa^{-1}, i.e., it is reduced by 52% at $p = 1$ GPa. The temperature dependence of n_s is best described by a two-gap s-wave model, with both superconducting gaps being decreased by hydrostatic pressure until the smaller gap completely disappears at $p = 1$ GPa.

DOI: 10.1103/PhysRevB.86.174516 PACS number(s): 74.70.Xa, 76.75.+i, 74.25.Ha, 74.20.Mn

I. INTRODUCTION

The antiferromagnetic $BaFe_2As_2$ is a mother compound of the "122" family of the iron-based arsenide unconventional superconductors. It crystallizes in the tetragonal $ThCr_2Si_2$ crystal structure with the space group of $I4/mmm$.[1] High-temperature superconductivity can be induced in this system by either isovalent substitution,[2–7] chemical charge carrier doping,[8,9] or hydrostatic pressure,[10–14] highlighting the great flexibility of the recently discovered iron-based superconductors to tune its electronic properties in general. The highest superconducting transition temperatures are achieved by hole doping in $Ba_{1-x}A_xFe_2As_2$ upon substituting Ba with A = K[8] or Rb,[15–17] with a gradual transition from the magnetically ordered ground state[18] towards a superconducting state as a function of x. The optimal superconducting transition temperature up to $T_c \simeq 38$ K is reached for $x \simeq 0.4$ in both cases.[8,17] Different hole and electron bands are crossing the Fermi level in the case of the optimally doped system as revealed by angle-resolved photoemission spectroscopy.[19–21] The topology of the Fermi surface is basically dominated by big hole bands around the Γ point and small electron bands at the M point, presenting favorable nesting conditions possibly related to the magnetic instabilities. This favorable topology is also thought to lead to interband processes playing an important role for the superconducting state.[22] The indication of multigap superconductivity in the hole-doped system $Ba_{1-x}Rb_xFe_2As_2$ was confirmed by our recent muon-spin spectroscopy (μSR) measurements.[17] Further hole doping reduces T_c down to 3.5 and 2.6 K for A = K and A = Rb,[23] for $x = 1$, and shifts the electron bands to the unoccupied side.[24] Therefore, one expects an absence of nesting conditions and hence of magnetic order, as confirmed, for example, by our μSR zero-field (ZF) measurements.[25] Another consequence is a strong decrease in the interband processes, which might be related to the collapse of T_c. Furthermore, it was found that the superfluid density for the end compound of the series, $RbFe_2As_2$, is much larger than in other Fe-based and unconventional superconductors.[17] This might signal a more conventional nature of the superconducting ground state. A further microscopic characterization of this compound seems highly mandatory since it may, in comparison with the optimally doped compounds from the same series, provide valuable information on the origin of high-T_c superconductivity in Fe-based materials. Therefore, we extended our earlier μSR studies on $RbFe_2As_2$ by performing measurements under hydrostatic pressure. Due to its comparatively low upper critical field, $B_{c2} = 2.6(1)$ T and its reduced $T_c = 2.52(2)$ K, this system allows the study of a large section of the B-T-p phase diagram. As exemplified by a number of recent studies, the μSR technique is very well suited to investigation of iron-based superconductors (see, for example, Ref. 26) and to provision of quantitative measures of several microscopic parameters of the superconducting ground state. Here we report the determination of T_c, the London penetration depth λ, and hence the superfluid density $n_s \propto \lambda^{-2}$, the superconducting gap values Δ, the upper critical field B_{c2}, and the Ginzburg-Landau parameter κ, as a function of the hydrostatic pressure. From our study it follows that the superconducting state in $RbFe_2As_2$ is indeed conventional and that hydrostatic pressure pushes it even further to the classical regime. Therefore a comparison of the electronic properties of $RbFe_2As_2$ under pressure with optimally doped members of the same family may provide essential information on the origin of the high-T_c phenomena in Fe-based superconductors.

II. EXPERIMENTAL DETAILS

The polycrystalline sample of $RbFe_2As_2$ used for the present experiment was synthesized in a two-step procedure at

the Laboratory for Solid State Physics of the ETH-Zürich.[16] First, RbAs and Fe_2As were prepared from pure elements in evacuated and sealed silica tubes. Then appropriate amounts of RbAs and Fe_2As were mixed, pressed into 8-mm-diameter pellets, and annealed at 650 °C for several days in evacuated and sealed silica ampoules. The quality was tested by x-ray diffraction and it was confirmed by our previous μSR studies at ambient pressure[25] that the sample is free of magnetic ordering. Then these cylindrical-shaped synthesized pellets, with a total height of 10 mm, were loaded into the CuBe pressure cell using Daphne oil as a pressure transfer medium. The ac susceptibility measurements were performed with a conventional lock-in amplifier at 0-, 0.27-, 0.46-, 0.68-, and 0.98-GPa pressures in the temperature interval of 1.4–10 K, using the same pressure cell as for μSR. Additional, magnetization data were obtained for pressures up to 5.4 GPa on a commercial Quantum Design 7-T Magnetic Property Measurement System XL SQUID Magnetometer using a homemade diamond anvil cell at temperatures between 1.8 and 10 K. Small lead (Pb) probes were used for pressure determination utilizing the pressure dependence of $T_{c,\mathrm{Pb}}$.[27]

The μSR measurements under pressure were performed at the μE1 beamline of the Paul Scherrer Institute (Villigen, Switzerland), using the GPD instrument equipped with an Oxford sorption pumped ^{3}He cryostat at temperatures down to 0.27 K. The pressure cells used during the μSR measurement and experimental setup are described elsewhere.[28,29] Data were collected at magnetic fields up to 0.25 T and for the three pressures 0.2, 0.6, and 1.0 GPa. Zero-pressure data are taken from our early experiments.[25] High-energy muons with a momentum of 105 MeV c^{-1} were used in order to penetrate the pressure cell walls. The typical statistics for both forward and backward detectors were 7 million. The fraction of muons stopping in the sample was about 45%, while the remaining fraction stops in the pressure cell. Three different transverse-field as well as ZF μSR measurements were done for each pressure point. The temperature dependence of the superfluid density was analyzed with the fitting package MUSRFIT developed by Suter and Wojek.[30]

III. RESULTS AND DISCUSSION

Figure 1 exibits the AC susceptibility data for pressure up to 1.0 GPa together with the pressure dependence of T_c. At ambient pressure the superconducting transition temperature of $RbFe_2As_2$ is $T_c = 2.55(2)$ K and it decreases linearly upon increasing the pressure with the rather large value of $dT_c/dp = -1.32$ K GPa^{-1}. A linear extrapolation of the data suggests that superconductivity could be completely suppressed by a pressure of approximately 2 GPa. In most superconductors, T_c is found to decrease under pressure, with some exceptions, as in the cuprate oxides or some iron-based systems, which exhibit a remarkable increase.[31,32] We note that a similarly large negative slope was found in another multigap superconductor, MgB_2, where T_c decreases under pressure at the rate of $dT_c/dp \simeq -1.11$ K GPa^{-1} (see Refs. 33 and 34).

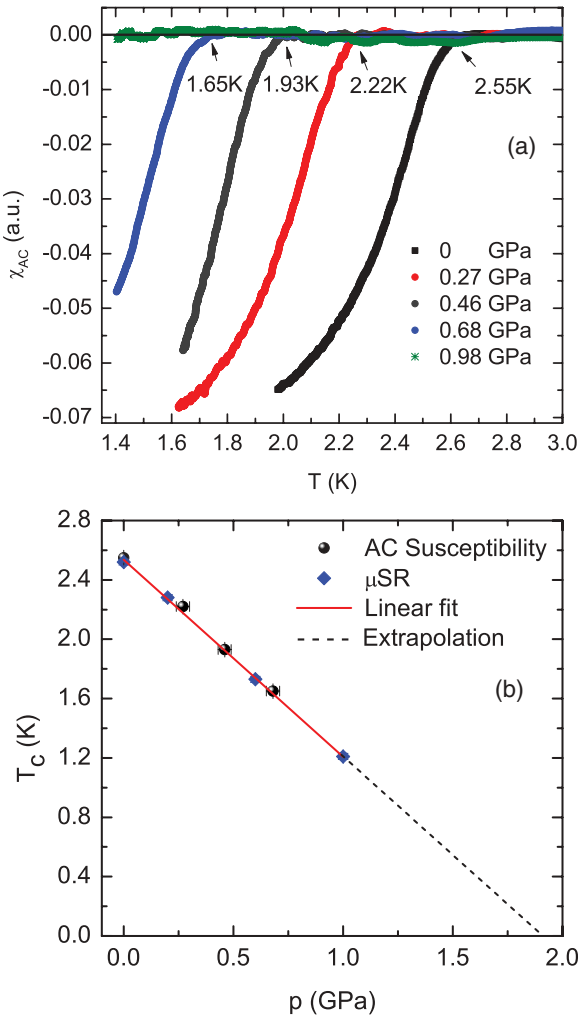

FIG. 1. (Color online) (a) The ac susceptibility measurements up to 1.0 GPa obtained with the same CuBe pressure cell as used for μSR experiments. (b) Pressure dependence of T_c. The solid (red) line corresponds to a linear fit, and the dashed (black) line is an extrapolation up to 1.92 GPa.

The time evolution of the μSR signal is best described by the polarization function,[28]

$$\begin{aligned} A_0 P(t) &= A_s \exp\left[-\frac{\left(\sigma_s^2+\sigma_n^2\right)}{2}t^2\right]\cos(\gamma_\mu B_{\mathrm{int}} t+\varphi) \\ &\quad + A_{\mathrm{pc}} \exp\left[-\frac{\sigma_{\mathrm{pc}}^2}{2}t^2\right]\int P(B_{\mathrm{pc}})\cos(\gamma_\mu B_{\mathrm{pc}} t+\varphi) dB_{\mathrm{pc}}, \end{aligned} \tag{1}$$

where the first term corresponds to the signal arising from the sample with the corresponding parameters: A_s, the initial asymmetry; σ_{sc}, the second moment of the magnetic-field distribution due to the flux line lattice in the mixed state; σ_n, the depolarization rate due to the nuclear moments; and B_{int}, the internal magnetic field at the muon site. The second term on the right-hand side of Eq. (1) represents the pressure cell contribution. A_{pc} denotes the initial asymmetry; $\sigma_{\mathrm{pc}} = 0.27\ \mu\mathrm{s}^{-1}$, the field- and temperature-independent Gaussian relaxation rate of the CuBe pressure cell material; and B_{pc} is

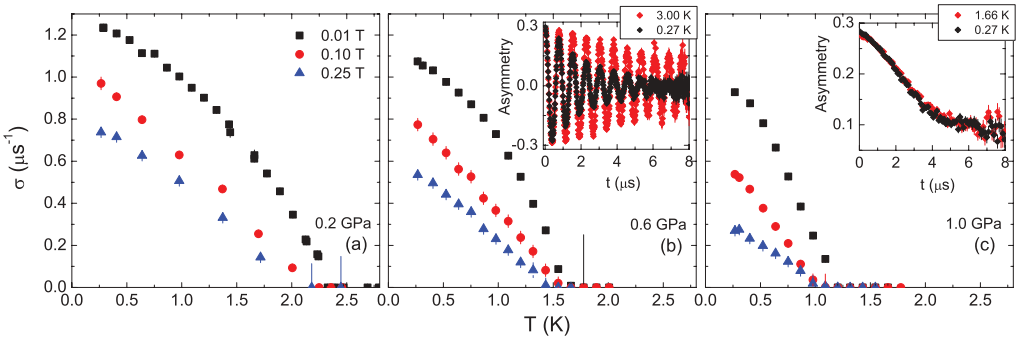

FIG. 2. (Color online) Temperature dependence of $\sigma_s(T)$ obtained for $RbFe_2As_2$ at different pressures. For each pressure, measurements at different fields were performed. Transverse-field [inset in (b)] and zero-field [inset in (c)] μSR time spectra above and below T_c at 1.0-GPa pressure.

the magnetic field sensed by the muons stopped in the pressure cell. $\gamma_\mu = 135.5342 \times 2\pi$ MHz T^{-1} is the muon gyromagnetic ratio and φ is the initial phase of the muon spin polarization. $P(B_{pc})$ is the distribution of magnetic fields sensed by the muons in the pressure cell, which is calculated using Eq. (A4) in Ref. 28. Therefore the integral is invoked to describe the sum of the applied field and the field induced by the sample in a diamagnetic state.

For each pressure point, ZF μSR measurements have been performed to check the magnetic properties of the system. No sign of magnetism, either static order or slow magnetic fluctuations, has been observed up to the highest pressure investigated in this study. This is illustrated by the ZF spectra at 1.0 GPa shown in the inset in Fig. 2(c).

The superconducting properties were investigated by transverse-field μSR measurements in the mixed state after field cooling, which ensures the formation of a uniform flux line lattice. Fitting Eq. (1) to the μSR time spectra, we obtain the temperature-, magnetic-field-, and pressure-dependent parameters $\sigma_{sc}(T,B,p)$ [see Figs. 2(a)–2(c)]. Using the numerical Ginzburg-Landau model developed by Brandt,[35]

$$\sigma_s\ [\mu s^{-1}] = 4.83 \times 10^4 (1 - B_{ext}/B_{c2}) \times [1 + 1.21(1 - \sqrt{B_{ext}/B_{c2}})^3]\lambda^{-2}\ [\text{nm}], \quad (2)$$

one can fit the field-dependent depolarization rate $\sigma_s(B_{ext})|_{T,\ p=\text{const}}$ and evaluate two important parameters of the superconducting state, i.e., the London penetration depth λ and the upper critical field B_{c2} (see Fig. 3). This approach assumes that λ is field independent, as confirmed by our previous zero-pressure measurements.[25]

As the second step, the temperature dependence of the superconducting carrier concentration $\rho_s = n_s(T)/n_s(0) = \lambda^{-2}(T)/\lambda^{-2}(0)$ is calculated from the inverse square of the penetration depth. It can be fitted using the local (London) approximation,[36]

$$\rho_s = \frac{\lambda^{-2}(T)}{\lambda^{-2}(0)} = 1 - \frac{2}{k_B T}\int_\Delta^\infty f(\epsilon,T)\,[1 - f(\epsilon,T)]\,d\epsilon, \quad (3)$$

leaving $\lambda^{-2}(0)$ and $\Delta(0)$ as free parameters. Here $f(\epsilon,T) = [1 + \exp(\sqrt{\epsilon^2 + \Delta(T)^2}/k_B T)]^{-1}$ represents the Fermi function with the BCS spherical s-wave type of $\Delta(T)$ gap.[30]

As evidenced by our previous study,[25] an $s+s$ multigap model,

$$\rho_s = \omega\rho_{s1} + (1 - \omega)\rho_{s2}, \quad (4)$$

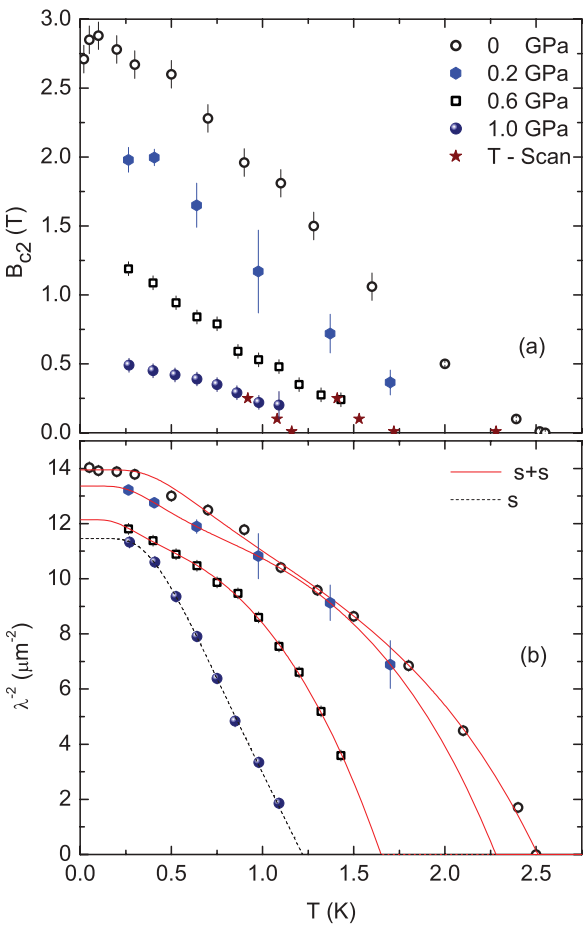

FIG. 3. (Color online) (a) Temperature and pressure dependence of the upper critical field $B_{c2}(T)$. Stars correspond to values obtained by analyzing the temperature dependence of $\sigma_s(T)$. Other symbols were obtained by fitting Eq. (2) to the $\sigma_s(B_{ext})|_{T,p=\text{const}}$ data. (b) Temperature and pressure dependence of λ^{-2} (in T). Solid lines correspond to an $s+s$–wave multigap fit model; dashed line, to an s-wave single-gap fit.

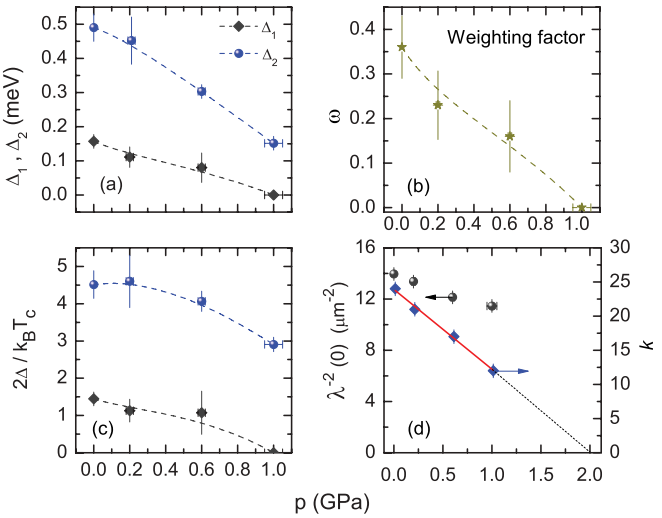

FIG. 4. (Color online) Pressure dependence of (a) the zero-temperature gap values $\Delta_1(0)$ and $\Delta_2(0)$, (b) the weight ω of the small gap, (c) the BCS ratios $2\Delta(0)/k_BT_c$ for both gaps, and (d) the inverse square of the penetration depth $\lambda^{-2}(0)$ and Ginzburg-Landau parameter k. Lines are guides for the eye.

where ω is the relative weighting factor for the smaller gap, $\Delta_1(0)$, gives a satisfactory fitting result which is also supported by ARPES measurements, where several disconnected Fermi-surface sheets are detected for another member of the 122 iron arsenide family.[20] The fitting results are shown in Fig. 3(b) and the pressure dependence of the parameters is reported in Fig. 4. It is found that the hydrostatic pressure only slightly reduces the superfluid density. Note that at 1.0 GPa, one does not require anymore the $s+s$ model and that a single s-wave gap scenario (i.e., $\omega \simeq 0$) is sufficient to describe the data. One may remark that upon increasing the hydrostatic pressure, the positive curvature of B_{c2}(T) near T_c gradually disappears and ends up with a usual BCS temperature dependence shape at 1.0 GPa [Fig. 3(a)], providing an additional indication of the disappearance of the smaller gap. Both gaps gradually decrease, and at 1.0 GPa the small gap Δ_1 essentially disappeared [Fig. 4(a)]; correspondingly, its weighting factor falls from a maximum $\omega = 0.36$ value to 0 [Fig. 4(b)]. The BCS ratios $2\Delta_1(0)/k_BT_c = 1.5(1)$ and $2\Delta_2(0)/k_BT_c = 4.5(1)$ are relatively independent of pressure up to 0.6 GPa, followed by a gradual drop for the large-gap value in the absence of the smaller gap. Upon increasing the hydrostatic pressure from 0 to 1.0 GPa, T_c is reduced by ~52%, while the superfluid density $\rho \propto \lambda^{-2}$ is decreased by only ~18%. In other words, as shown in Fig. 4(d), the superfluid density only weakly depends on the hydrostatic pressure, in contrast to the strong dependence of T_c, typical for unconventional high-T_c superconductors, where a proportionality of these two quantities is usually observed (at least in under- and optimally doped compounds). Using the pressure-dependent values of the penetration depths and upper critical field, one can determine the characteristic ratio, known as the Ginzburg-Landau parameter, $\kappa = \lambda/\xi$, determined at our base temperature of 0.27 K.[36] ξ is a superconducting coherent length calculated from the relation $B_{c2} = \Phi_0/2\pi\xi^2$, where $\Phi_0 = 2.0678 \times 10^{-15}$ Wb is the magnetic flux quantum. A reduction of κ by 50% is determined at the highest available pressure in this experiment, pointing to a clear shift of the superconducting character of $RbFe_2As_2$ away from a strong type II superconductor towards a low-κ classical BCS superconductor. Interestingly, both T_c and κ linearly decrease with pressure and therefore we find the experimental correlation $\kappa \propto T_c$ (see Table I).

TABLE I. List of the pressure dependent parameters obtained from the analysis of $\lambda^{-2}(T)$.

p (GPa)	T_c (K)	$\Delta_1(0)$ (meV)	$\Delta_2(0)$ (meV)	$\frac{2\Delta_1(0)}{k_BT_c}$	$\frac{2\Delta_2(0)}{k_BT_c}$	κ	$\lambda(0)$ (nm)
0.00(0)	2.52(2)	0.15(2)	0.49(4)	1.5(2)	4.5(4)	24(1)	267(5)
0.20(1)	2.28(1)	0.11(3)	0.45(7)	1.1(3)	4.6(7)	21(1)	274(5)
0.60(1)	1.73(1)	0.08(4)	0.30(2)	1.1(6)	4.1(3)	17(1)	287(6)
1.00(2)	1.21(1)	0.00(0)	0.15(1)	0.0(0)	2.9(2)	12(1)	295(6)

One way to visualize and to shed light on the nature of the superconducting state has been presented by Uemura *et al.* in Refs. 37 and 38. According to the so-called "Uemura plot" the universal linear relation between T_c and $\sigma_s(T \to 0)$ has been found for high-temperature superconductor cuprates. The critical temperature appears to be proportional to the inverse square of the London penetration depth $T_c \propto \rho_s \propto \lambda^{-2}$ for a large number of cuprate superconductors, but the proportionality constant is different for hole- and electron-doped superconductors.[39] A number of Fe-based superconductors appear to follow the Uemura relation (see Fig. 5). For comparative purposes we include the data points for $RbFe_2As_2$ in the Uemura plot. As evidenced by Fig. 5, various families of unconventional superconductors including high-T_c Fe-based materials are characterized by low λ^{-2} values (superfluid density) compared to their T_c; i.e., they exhibit a dilute superfluidity. In contrast, conventional phonon-mediated

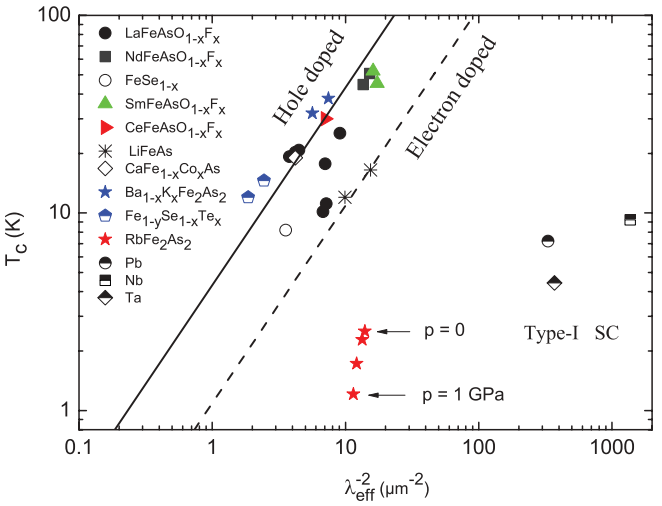

FIG. 5. (Color online) Uemura plot for some Fe-based high-temperature superconductors. The Uemura relation observed for underdoped cuprates is shown as a dashed (black) line for electron doping and as a solid line for hole doping.[39] Data are taken from the following references: $LaFeAsO_{1-x}F_x$;[44–47] $NdFeAs_{1-x}F_x$;[47,48] $FeSe_{1-x}$;[49,50] $SmFeAs_{1-x}F_x$;[48,51] $CeFeAs_{1-x}F_x$;[47] LiFeAs;[52] $CaF_{1-x}Co_xFe_2As_2$;[53] $Ba_{1-x}K_xFe_2As_2$;[21] $Fe_{1-y}Se_{1-x}Te_x$;[54,55] Pb, Nb, and Ta;[56] $RbFe_2As_2$, this work and Ref. 25.

superconductors like elemental metals possess a dense superfluid and exhibit low values of T_c. $RbFe_2As_2$ falls in between these two extreme cases. With increased hydrostatic pressure the critical temperature decreases rapidly, compared to the superfluid density, and the relation of T_c to λ^{-2} moves closer to the one characteristic of conventional superconductors.

In the following, we discuss the different effects of hydrostatic pressure and reduction of the lattice parameters by substitution with smaller ions on the $RbFe_2As_2$ system. As mentioned above, the related compound KFe_2As_2 is also superconducting, with an increased $T_c = 3.8$ K, compared to $T_c = 2.6$ K for $RbFe_2As_2$. Due to the smaller ionic radius of K^+ compared to Rb^+, both the a- and the c-axis parameters of KFe_2As_2 are reduced.[8,15,18,23,40] In other words, in the up-to-now-hypothetical series $Rb_{1-y}K_yFe_2As_2$, the shrinkage of lattice with increasing y should finally lead to the experimentally observed increased T_c. In sharp contrast, our hydrostatic pressure experiments on $RbFe_2As_2$ show a strong reduction of T_c with increasing pressures. A possible way out of the apparent discrepancy could be a nonmonotonic dependence of T_c on pressure with a reappearance of superconductivity at higher pressures, as recently observed in another Fe-based superconductor.[41,42] Therefore, we tested this hypothesis by performing further magnetization studies under high pressure using a diamond anvil cell. No superconducting transition was detected above 1.8 K up to our maximum pressure of 5.4 GPa. Based on these experimental facts, one has to conclude that the external pressure is not simply equivalent to a reduction of the lattice parameters in this particular compound. This is probably related to the different effects of the two forms of pressure on the local atomic structure within the FeAs tetrahedra, which is known to be one of the governing parameters determining the T_c in Fe-based superconductors.[43]

IV. SUMMARY AND CONCLUSION

To summarize, μSR and magnetization measurements under hydrostatic pressures (0.2, 0.6, and 1.0 GPa) were carried out on the polycrystalline $RbFe_2As_2$ hole-overdoped iron-based superconductor. A negative pressure effect was observed on the critical temperature, at the rate of $dT_c/dp = -1.32$ K GPa^{-1}, in contrast to the positive effect expected for an equivalency of chemical and hydrostatic pressures. The zero-temperature values of the London penetration depth $\lambda(0)$, superconducting gaps $\Delta(0)$, upper critical field B_{c2}, and Ginzburg-Landau parameter $\kappa = \lambda/\xi$ have been evaluated from the experimental data. The superfluid density was found to be weakly pressure dependent, while κ and T_c are linearly reduced by 50% by the application of pressures up to 1 GPa. Upon increasing the hydrostatic pressure, the system undergoes a transition from an $s + s$–wave multigap superconducting state to a single-s-wave gap state.

Here, one can highlight three main points in favor of the tendency to the conventional BCS type of superconductors.

(1) Upon increasing the hydrostatic pressure, the $RbFe_2As_2$ compound exhibits a gradual transition from a two-gap to a single-gap state, ending up with the BCS ratio of $2\Delta/k_BT_c = 2.9(2)$.

(2) A strong reduction of κ, from 24 down to 12, is observed, getting closer to that for the conventional BCS superconductors, and in the limit of high pressures it extrapolates to a value typical for the type I superconductors.

(3) The Uemura classification scheme shows that with increased hydrostatic pressure, the critical temperature reduces more rapidly than the superfluid density, and the relation of T_c to λ^{-2} moves closer to the region where a low critical temperature and a high superfluid density are characteristics of conventional superconductors.

Moreover, n_s is only diminished by 18% at $p = 1$ GPa, indicating that the proportionality of n_s and T_c found for several families of under- and optimally doped unconventional superconductors does not hold for $RbFe_2As_2$ either. On the other hand, these observations are rather typical for classical low-temperature BCS superconductors.[57] In addition, the temperature dependence of n_s is best described by a two-gap s-wave model, with both superconducting gaps being decreased by hydrostatic pressure until the smaller gap completely disappears at 1 GPa. Hence, the hydrostatic pressure appears to shift the nature of the ground state of the hole-overdoped $RbFe_2As_2$ system to an even more classical superconducting state. The superconducting ground state of the hole-overdoped $RbFe_2As_2$ system appears to be rather conventional. Since no superconducting transition was detected above 1.8 K up to 5.4-GPa pressure, one may conclude that the external pressure is not equivalent to the reduction of lattice parameters in this particular compound. Experimental and theoretical comparisons of the electronic properties of $RbFe_2As_2$ under pressure with optimally doped members of the same family should therefore provide new insight into the origin of the high-T_c phenomena in Fe-based superconductors.

ACKNOWLEDGMENTS

The μSR and magnetization experiments up to 1.0 GPa were performed at the Swiss Muon Source, Paul Scherrer Institute, Villigen, Switzerland. We acknowledge support by the Swiss National Science Foundation and the NCCR Materials with Novel Electronic Properties (MaNEP).

*Correspondence author: zurab.shermadini@psi.ch

[1] M. Pfisterer and G. Nagorsen, Z. Naturforsch. B **35**, 703 (1980).
[2] S. Jiang, H. Xing, G. Xuan, C. Wang, Z. Ren, C. Feng, J. Dai, Z. Xu, and G. Cao, J. Phys.: Condens. Matter **21**, 382203 (2009).
[3] S. Kasahara, T. Shibauchi, K. Hashimoto, K. Ikada, S. Tonegawa, R. Okazaki, H. Shishido, H. Ikeda, H. Takeya, K. Hirata *et al.*, Phys. Rev. B **81**, 184519 (2010).
[4] W. Cao *et al.*, Europhys. Lett. **86**, 47002 (2009).
[5] K. Hashimoto, S. Kasahara, R. Katsumata, Y. Mizukami, M. Yamashita, H. Ikeda, T. Terashima, A. Carrington, Y. Matsuda, and T. Shibauchi, Phys. Rev. Lett. **108**, 047003 (2012).
[6] Y. Qi, L. Wang, Z. Gao, D. Wang, X. Zhang, and Y. Ma, Physica C **469**, 1921 (2009).
[7] Z. R. Ye, Y. Zhang, F. Chen, M. Xu, Q. Q. Ge, J. Jiang, B. P. Xie, and D. L. Feng, Phys. Rev. B **86**, 035136 (2012).

[8]M. Rotter, M. Tegel, and D. Johrendt, Phys. Rev. Lett. **101**, 107006 (2008).
[9]Y. Kamihara *et al.*, Am. Chem. Soc. **130**, 3296 (2008).
[10]H. Takahashi, K. Igawa, K. Arii, Y. Kamihara, M. Hirano, and H. Hosono, Nature (London) **453**, 376 (2008).
[11]Y. Mizuguchi, F. Tomioka, S. Tsuda, T. Yamaguchi, and Y. Takano, Appl. Phys. Lett. **93**, 152505 (2008).
[12]A. D. Zocco, J. J. Hamlin, R. E. Baumbach, M. B. Maple, M. A. McGuire, A. S. Sefat, B. C. Sales, R. Jin, D. Mandrus, J. R. Jeffries *et al.*, Physica C **468**, 2229 (2008).
[13]J. J. Hamlin, R. E. Baumbach, D. A. Zocco, T. A. Sayles, and M. B. Maple, J. Phys.: Condens. Matter **20**, 365220 (2008).
[14]H. Okada, K. Igawa, H. Takahashi, Y. Kamihara, M. Hirano, H. Hosono, K. Matsubayashi, and Y. Uwatoko, J. Phys. Soc. Jpn. **77**, 113712 (2008).
[15]Z. Bukowski, S. Weyeneth, R. Puzniak, P. Moll, S. Katrych, N. D. Zhigadlo, J. Karpinski, H. Keller, and B. Batlogg, Phys. Rev. B **79**, 104521 (2009).
[16]Z. Bukowski *et al.*, Physica C **470**, S328 (2010).
[17]Z. Guguchia, Z. Shermadini, A. Amato, A. Maisuradze, A. Shengelaya, Z. Bukowski, H. Luetkens, R. Khasanov, J. Karpinski, and H. Keller, Phys. Rev. B **84**, 094513 (2011).
[18]M. Rotter, M. Tegel, D. Johrendt, I. Schellenberg, W. Hermes, and R. Pöttgen, Phys. Rev. B **78**, 020503 (2008).
[19]V. B. Zabolotnyy *et al.*, Nature **457**, 569 (2009).
[20]D. V. Evtushinsky *et al.*, New J. Phys. **11**, 055069 (2009).
[21]R. Khasanov, D. V. Evtushinsky, A. Amato, H.-H. Klauss, H. Luetkens, C. Niedermayer, B. Büchner, G. L. Sun, C. T. Lin, J. T. Park *et al.*, Phys. Rev. Lett. **102**, 187005 (2009).
[22]H. Ding *et al.*, J. Phys.: Condens. Matter **23**, 135701 (2011).
[23]K. Sasmal, B. Lv, B. Lorenz, A. M. Guloy, F. Chen, Y.-Y. Xue, and C.-W. Chu, Phys. Rev. Lett. **101**, 107007 (2008).
[24]T. Sato, K. Nakayama, Y. Sekiba, P. Richard, Y.-M. Xu, S. Souma, T. Takahashi, G. F. Chen, J. L. Luo, N. L. Wang *et al.*, Phys. Rev. Lett. **103**, 047002 (2009).
[25]Z. Shermadini, J. Kanter, C. Baines, M. Bendele, Z. Bukowski, R. Khasanov, H.-H. Klauss, H. Luetkens, H. Maeter, G. Pascua *et al.*, Phys. Rev. B **82**, 144527 (2010).
[26]A. Amato *et al.*, Physica C **469**, 606 (2009).
[27]A. Eiling and J. S. Schilling, J. Phys. F **11**, 623 (1981).
[28]A. Maisuradze, A. Shengelaya, A. Amato, E. Pomjakushina, and H. Keller, Phys. Rev. B **84**, 184523 (2011).
[29]D. Andreica, Ph.D. thesis, IPP/ETH-Zurich (2001).
[30]A. Suter and B. M. Wojek, Phys. Procedia **30**, 69 (2012).
[31]M. K. Wu, J. R. Ashburn, C. J. Torng, P. H. Hor, R. L. Meng, L. Gao, Z. J. Huang, Y. Q. Wang, and C. W. Chu, Phys. Rev. Lett. **58**, 908 (1987).
[32]L. Gao, Y. Y. Xue, F. Chen, Q. Xiong, R. L. Meng, D. Ramirez, C. W. Chu, J. H. Eggert, and H. K. Mao, Phys. Rev. B **50**, 4260 (1994).
[33]S. Deemyad, T. Tomita, J. J. Hamlin, B. R. Beckett, J. S. Schilling, D. G. Hinks, J. D. Jorgensen, S. Lee, and S. Tajima, Physica C **385**, 105 (2003).
[34]J. S. Schilling, *A Treatise on Theory and Applications*, edited by J. R. Schrieffer (Springer-Verlag, Hamburg, 2006).
[35]E. H. Brandt, Phys. Rev. B **68**, 054506 (2003).
[36]M. Tinkham, *Introduction to Superconductivity* (McGraw–Hill, New York, 1996).
[37]Y. J. Uemura, L. P. Le, G. M. Luke, B. J. Sternlieb, W. D. Wu, J. H. Brewer, T. M. Riseman, C. L. Seaman, M. B. Maple, M. Ishikawa *et al.*, Phys. Rev. Lett. **66**, 2665 (1991).
[38]Y. J. Uemura, G. M. Luke, B. J. Sternlieb, J. H. Brewer, J. F. Carolan, W. N. Hardy, R. Kadono, J. R. Kempton, R. F. Kiefl, S. R. Kreitzman *et al.*, Phys. Rev. Lett. **62**, 2317 (1989).
[39]A. Shengelaya, R. Khasanov, D. G. Eshchenko, D. Di Castro, I. M. Savić, M. S. Park, K. H. Kim, S.-I. Lee, K. A. Müller, and H. Keller, Phys. Rev. Lett. **94**, 127001 (2005).
[40]M. Rotter *et al.*, Chem. Int. Ed. **47**, 7949 (2008).
[41]J. Guo, X.-J. Chen, J. Dai, C. Zhang, J. Guo, X. Chen, Q. Wu, D. Gu, P. Gao, L. Yang *et al.*, Phys. Rev. Lett. **108**, 197001 (2012).
[42]L. Sun *et al.*, Nature **483**, 67 (2012).
[43]Y. Mizuguchi *et al.*, Supercond. Sci. Technol. **23**, 054013 (2010).
[44]H. Luetkens, H.-H. Klauss, R. Khasanov, A. Amato, R. Klingeler, I. Hellmann, N. Leps, A. Kondrat, C. Hess, A. Köhler *et al.*, Phys. Rev. Lett. **101**, 097009 (2008).
[45]H. Luetkens *et al.*, Nat. Mater. **8**, 305 (2009).
[46]S. Takeshita *et al.*, New J. Phys. **11**, 035006 (2009).
[47]J. P. Carlo, Y. J. Uemura, T. Goko, G. J. MacDougall, J. A. Rodriguez, W. Yu, G. M. Luke, P. Dai, N. Shannon, S. Miyasaka *et al.*, Phys. Rev. Lett. **102**, 087001 (2009).
[48]R. Khasanov, H. Luetkens, A. Amato, H.-H. Klauss, Z.-A. Ren, J. Yang, W. Lu, and Z.-X. Zhao, Phys. Rev. B **78**, 092506 (2008).
[49]R. Khasanov, M. Bendele, A. Amato, K. Conder, H. Keller, H.-H. Klauss, H. Luetkens, and E. Pomjakushina, Phys. Rev. Lett. **104**, 087004 (2010).
[50]R. Khasanov, K. Conder, E. Pomjakushina, A. Amato, C. Baines, Z. Bukowski, J. Karpinski, S. Katrych, H.-H. Klauss, H. Luetkens *et al.*, Phys. Rev. B **78**, 220510 (2008).
[51]A. J. Drew, F. L. Pratt, T. Lancaster, S. J. Blundell, P. J. Baker, R. H. Liu, G. Wu, X. H. Chen, I. Watanabe, V. K. Malik *et al.*, Phys. Rev. Lett. **101**, 097010 (2008).
[52]F. L. Pratt, P. J. Baker, S. J. Blundell, T. Lancaster, H. J. Lewtas, P. Adamson, M. J. Pitcher, D. R. Parker, and S. J. Clarke, Phys. Rev. B **79**, 052508 (2009).
[53]S. Takeshita, R. Kadono, M. Hiraishi, M. Miyazaki, A. Koda, S. Matsuishi, and H. Hosono, Phys. Rev. Lett. **103**, 027002 (2009).
[54]H. Kim, C. Martin, R. T. Gordon, M. A. Tanatar, J. Hu, B. Qian, Z. Q. Mao, R. Hu, C. Petrovic, N. Salovich *et al.*, Phys. Rev. B **81**, 180503 (2010).
[55]M. Bendele, S. Weyeneth, R. Puzniak, A. Maisuradze, E. Pomjakushina, K. Conder, V. Pomjakushin, H. Luetkens, S. Katrych, A. Wisniewski *et al.*, Phys. Rev. B **81**, 224520 (2010).
[56]A. Suter, E. Morenzoni, N. Garifianov, R. Khasanov, E. Kirk, H. Luetkens, T. Prokscha, and M. Horisberger, Phys. Rev. B **72**, 024506 (2005).
[57]R. Khasanov, P. S. Häfliger, N. Shitsevalova, A. Dukhnenko, R. Brütsch, and H. Keller, Phys. Rev. Lett. **97**, 157002 (2006).